Theory of a quantum critical phenomenon in a topological insulator: (3 + 1)-dimensional quantum electrodynamics in solids

Hiroki Isobe[1] and Naoto Nagaosa[1,2]

[1]*Department of Applied Physics, University of Tokyo, Tokyo 113-8656, Japan*

[2]*Cross Correlated Materials Research Group (CMRG) and Correlated Electron Research Group (CERG), ASI, RIKEN, Wako, Saitama 351-0198, Japan*

(Received 11 May 2012; revised manuscript received 3 October 2012; published 19 October 2012)

We study theoretically the quantum critical phenomenon of the phase transition between the trivial insulator and the topological insulator in $(3+1)$ dimensions, which is described by a Dirac fermion coupled to the electromagnetic field. The renormalization group (RG) equations for the running coupling constant α, the speed of light c, and electron v are derived. The almost exact analytic solutions to these RG equations are obtained to reveal that (i) c and v approach to the common value with combination c^2v being almost unrenormalized, (ii) the RG flow of α is the same as that of usual QED with c^3 being replaced by c^2v, and (iii) there are two crossover momentum/energy scales separating three regions of different scaling behaviors. The dielectric and magnetic susceptibilities, angle-resolved photoemission spectroscopy (ARPES), and the behavior of the gap are discussed from this viewpoint.

DOI: 10.1103/PhysRevB.86.165127 PACS number(s): 73.43.Nq, 64.70.Tg, 71.10.−w

I. INTRODUCTION

In solids, the electronic states are described by the Bloch wave functions with the energy dispersion $\varepsilon_n(\vec{k})$ where n being the band index and $\vec{k}$ the crystal momentum. The velocity of electrons given by $\vec{v}_n(\vec{k}) = \partial\varepsilon_n(\vec{k})/\partial\vec{k}$ is usually much smaller than that of light c. Therefore, the Lorentz invariance is terribly broken and hence many of the beautiful results in quantum electrodynamics (QED)[1] are not applicable to the Bloch electrons in solids. The smallness of the factor $v_n(\vec{k})/c \ll 1$ naturally leads to the gauge choice (i.e., Coulomb gauge) where the scalar potential gives the Coulomb interaction without retardation while the electron-electron interaction through the transverse part of the vector potential $\vec{A}$ is often neglected. The latter is often treated as the external electromagnetic field for the probe of the electromagnetic response of the system. This gauge choice is regarded as the "physical gauge." For example, one can discuss the physical meaning of the Green's function $G(\vec{k},\omega)$ in this gauge where the quasiparticle corresponds its pole structure. Angle-resolved photoemission spectroscopy (ARPES) is also formulated in this gauge [i.e., ARPES intensity is proportional to the electron spectrum function $-\mathrm{Im}G(\vec{k},\omega)$].[2]

While the nonrelativistic quantum mechanics is basically justified for the electrons in solids, there are some cases where the Dirac fermions appear in the electronic band structure. A representative case is graphene, a two-dimensional sheet of carbon network with hexagonal lattice, where the 2×2 Dirac spectrum near K and K' points describes the low-energy physics.[3] Another example is Bi, which is described by 4×4 Dirac fermions and shows the enhanced orbital diamagnetism.[4] Recent advances in this field are the discovery of the topological insulator and its associated quantum phase transition.[5,6] The relativistic spin-orbit interaction (SOI) rearrange the spin states to yield the "twist" of the Bloch wave functions in the first Brillouin zone. This twist is characterized by the Z_2 topological integer. In general, topological integers can change only discontinuously when the gap closes, which can be described by the local Hamiltonian in k space. When the inversion symmetry exists, the effective Hamiltonian near this quantum phase transition is the Dirac Hamiltonian expanded around the time-reversal invariant momentum (TRIM) $\vec{k}_0$ ($\vec{k}_0$ is equivalent to $-\vec{k}_0$). In this case, the orbitals and spins are coupled to form the 4×4 Dirac Hamiltonian and the sign change of the mass m corresponds to the quantum phase transition between trivial insulator and topological insulator. This story is actually realized in the materials such as $\mathrm{BiTl}(\mathrm{S}_{1-x}\mathrm{Se}_x)_2$ by changing the concentration x.[7,8]

The effects of the electron-electron interaction on the Dirac electrons are also extensively studied.[9–12] For graphene, it has been revealed that the electron speed v is renormalized to increase logarithmically by the long-range Coulomb interaction, while the coupling α is marginally irrelevant.[9] When the exchange of the transverse part of the vector potential is taken into account, the velocity v saturates to that of light c (i.e., the Lorentz invariance is recovered) and α remains finite in the infrared limit. This leads to an intriguing non-Fermi liquid state in $(2+1)$ dimensions.[10] For the $(3+1)$-dimensional [$(3+1)$D] case, the Coulomb interaction also gives the logarithmic enhancement of the velocity v and the coupling constant α is marginally irrelevant.[11,12] The disorder potential is irrelevant perturbatively, while the strong enough disorder drives the system toward the compressible diffusive metal (CDM).[11,13] However, the effect of the transverse part of the vector potential in $(3+1)$ dimensions has not yet been studied to the best of our knowledge.

In this paper, we study the quantum critical phenomenon of topological phase transition in $(3+1)$ dimensions. The Coulomb interaction as well as the transverse current-current interaction are considered.

II. DIRAC FERMIONS IN (3 + 1) DIMENSIONS IN ABSENCE OF LORENTZ INVARIANCE

A. Model

We start with the following Lagrangian:[14]

$$\mathcal{L} = \bar{\psi}(\gamma^0 p_0 - v\vec{\gamma}\cdot\vec{p} - m)\psi + \frac{1}{2}\left(\varepsilon\vec{E}^2 - \frac{1}{\mu}\vec{B}^2\right) - e\bar{\psi}\gamma^0\psi A_0 - e\frac{v}{c}\bar{\psi}\gamma^\alpha\psi A_\alpha, \quad (1)$$

where α is a spatial index ($\alpha = 1,2,3$) and $\gamma^\alpha p_\alpha = -\vec{\gamma}\cdot\vec{p}$. For the moment, we consider the critical point (i.e., $m = 0$). The renormalization of the mass m will be discussed later. The speed of light in material c and in vacuum $c_{\text{vacuum}} = 3\times10^8$ m/s are related through the permittivity ε and the permeability μ by $c^2 = c_{\text{vacuum}}^2/(\varepsilon\mu)$. We use a $(+---)$ metric. The electric field and magnetic field are represented in terms of the photon field A_μ as

$$\vec{E} = -\frac{1}{c}\frac{\partial\vec{A}}{\partial t} - \vec{\nabla}A_0, \quad \vec{B} = \frac{1}{c}\vec{\nabla}\times\vec{A}.$$

The electron propagator $G_0(p)$, the photon propagator $D_0^{\mu\nu}(p)$ and the vertex are given by

$$G_0(p) = \frac{i}{\gamma^0 p_0 + v\gamma^\alpha p_\alpha + i0}, \quad (2)$$

$$D_0^{\mu\nu}(q) = \frac{-ig^{\mu\nu}}{\varepsilon(q_0^2 - c^2q_\alpha^2) + i0}, \quad (3)$$

$$\text{vertex} = -ie\gamma^0 \quad \text{or} \quad -ie\frac{v}{c}\gamma^\alpha. \quad (4)$$

Here we employ the Feynman gauge because physical quantities are independent of gauge choice.

B. Perturbative renormalization group analysis

Calculations are performed by using dimensional regularization not to violate the gauge invariance of the theory. We set the space-time dimension $d = 4 - \epsilon$ to regularize divergences. The self-energy $\Sigma(p)$, polarization $\Pi_2^{\mu\nu}(q)$, and the vertex correction $\delta\Gamma^\mu(p',p)$ all to one-loop order (Fig. 1) are obtained as follows:

$$\Sigma(p) = \frac{e^2/\varepsilon}{4\pi^2\epsilon}\frac{1}{(c+v)^2c}\left[1 - 3\left(\frac{v}{c}\right)^2\right]\gamma^0 p_0 + \frac{e^2/\varepsilon}{12\pi^2\epsilon}\frac{2c+v}{(c+v)^2cv}\left[1 + \left(\frac{v}{c}\right)^2\right]v\vec{\gamma}\cdot\vec{p}, \quad (5)$$

$$\Pi_2^{\mu\nu}(q) = (q^2g^{\mu\nu} - q^\mu q^\nu)\left(\frac{v}{c}\right)^{2-\delta_{\mu0}-\delta_{\nu0}}\frac{1}{v^3}\Pi_2(q), \quad (6)$$

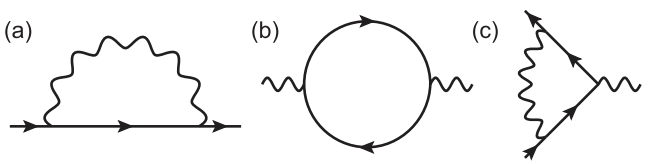

FIG. 1. Feynman diagrams considered here: (a) self-energy, (b) polarization, (c) vertex.

where

$$\Pi_2(q) = -\frac{e^2}{6\pi^2\epsilon} + O(\epsilon^0),$$

and

$$\delta\Gamma^0(0,0) = -\frac{e^2/\varepsilon}{4\pi^2\epsilon}\frac{1}{(c+v)^2c}\left[1 - 3\left(\frac{v}{c}\right)^2\right]\gamma^0, \quad (7a)$$

$$\delta\Gamma^\alpha(0,0) = \frac{e^2/\varepsilon}{12\pi^2\epsilon}\frac{2c+v}{(c+v)^2cv}\left[1 + \left(\frac{v}{c}\right)^2\right]\frac{v}{c}\gamma^\alpha. \quad (7b)$$

Comparing the result of the vertex correction Eq. (7) with the self-energy Eq. (5), we can confirm that the Ward-Takahashi identity is satisfied to one-loop order.

The diverging quantities appearing through the calculation of the one-loop diagrams are absorbed by rescaling some quantities. We can write the renormalized Lagrangian in the form

$$\mathcal{L} = \bar{\psi}(Z_{2t}\gamma^0 k_0 + Z_{2s}v\gamma^\alpha p_\alpha)\psi + \frac{1}{2}\left(Z_{3e}\varepsilon\vec{E}^2 - Z_{3m}\frac{1}{\mu}\vec{B}^2\right) - eZ_{1t}\bar{\psi}\gamma^0\psi A_0 - eZ_{1s}\frac{v}{c}\bar{\psi}\gamma^\alpha\psi A_\alpha. \quad (8)$$

Then we obtain the following RG equations using a momentum scale κ:

$$\kappa\frac{dv}{d\kappa} = -\frac{e^2/\varepsilon}{6\pi^2}\frac{1}{(c+v)^2}\left[1 + 2\left(\frac{v}{c}\right) + \left(\frac{v}{c}\right)^2 - 4\left(\frac{v}{c}\right)^3\right], \quad (9)$$

$$\kappa\frac{dc}{d\kappa} = \frac{e^2/\varepsilon}{12\pi^2}\frac{c^2 - v^2}{c^3v}, \quad (10)$$

$$\kappa\frac{d(e^2/\varepsilon)}{d\kappa} = \frac{(e^2/\varepsilon)^2}{6\pi^2}\frac{1}{c^2v}. \quad (11)$$

The coupling constant α is defined by $\alpha = e^2/(\varepsilon c^2 v)$. The numerical solutions for the RG equations are shown in Fig. 2 for the initial (bare) values of $v_0 = 0.01$, $c_0 = 0.5$, and $\alpha_0 = 1$.

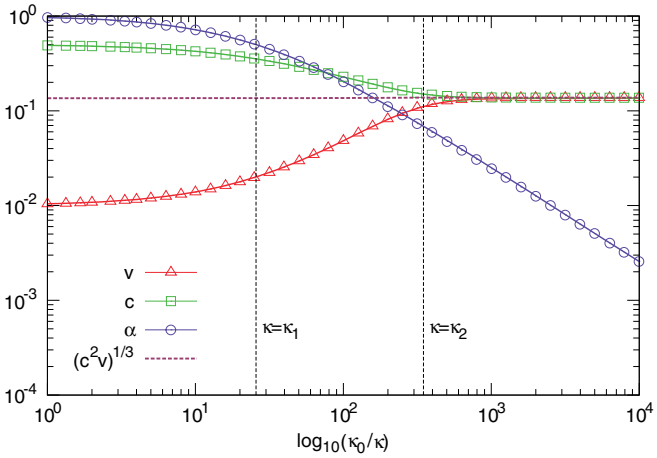

FIG. 2. (Color online) Solution to the RG equations for v, c, and α. We set the initial values $v_0 = 0.01$, $c_0 = 0.5$, and $\alpha_0 = 1$. For v, c, and α, the analytic solutions (solid lines) show a very good agreement with the numerical solutions (points). The dashed line for c^2v, obtained numerically, is almost constant for all momentum scale.

The result shows some important features. First, we can see that the quantity c^2v is almost constant for all momentum scales and remains $c_0^2v_0$. This fact enables the approximate but accurate analysis of the scaling functions as described below. Second, the speed of electron v and that of photon c approach to the same value $c_\infty = (c_0^2v_0)^{1/3}$ in the infrared (IR) limit. Third, the coupling constant α becomes small in the IR region, which justifies our perturbative RG analysis. Therefore, the quantum critical phenomenon of 3D topological insulator is an ideal laboratory to study the QED in a solid, even though the Lorentz invariance is broken to a large extent in the original (bare) Lagrangian.

C. Analytic solutions

Now we study the solution to the RG equation in more detail. The approximate relation $c^2v = c_0^2v_0$ makes the analysis much easier, and we can obtain the analytic solution. By replacing c^2v by $c_0^2v_0$, the RG equation for e^2/ε [Eq. (11)] is exactly the same as in the conventional QED. Therefore, the RG equation for the coupling constant α is

$$\kappa\frac{d\alpha}{d\kappa} = \frac{\alpha^2}{6\pi^2}, \tag{12}$$

and its solution is obtained as

$$\alpha(\kappa) = \frac{\alpha_0}{1+\frac{\alpha_0}{6\pi^2}\ln\left(\frac{\kappa_0}{\kappa}\right)}, \tag{13}$$

where κ_0 is the momentum cutoff. This approximate solution fits the numerical solution very well as shown in Fig. 2. The precision of the analytic solution is discussed in Appendix.

With $\alpha(\kappa)$ being obtained, one can solve the RG equation (10) for c as

$$c^6(\kappa) - c_0^4v_0^2 = \left(c_0^6 - c_0^4v_0^2\right)\left[1+\frac{\alpha_0}{6\pi^2}\ln\left(\frac{\kappa_0}{\kappa}\right)\right]^{-3}. \tag{14}$$

and $v(\kappa) = c_0^2v_0/[c(\kappa)]^2$. These analytic solutions are again compared with the numerical solutions in Fig. 2, and a good agreement is obtained.

Here we can identify the two momentum scales, κ_1 and κ_2. κ_1 is defined as the scale where the renormalization effect becomes appreciable [i.e., $\frac{\alpha_0}{6\pi^2}\ln(\frac{\kappa_0}{\kappa_1}) \cong 1$]. The second one κ_2 is defined as $c(\kappa_2) \cong v(\kappa_2)$ (i.e., the two velocities approaches to each other). These two scales are estimated as

$$\kappa_1 = \exp\left[-\frac{6\pi^2}{\alpha_0}\right]\kappa_0, \tag{15a}$$

$$\kappa_2 = \exp\left[-\frac{6\pi^2}{\alpha_0}\left(\frac{c_0}{v_0}\right)^{2/3}\right]\kappa_0, \tag{15b}$$

and $\kappa_2 \ll \kappa_1 \ll \kappa_0$, assuming $\alpha_0/(6\pi^2) \ll 1$ and $v_0/c_0 \ll 1$. These two momenta separate the three regions: (i) perturbative region $\kappa_1 \ll k \ll \kappa_0$, the renormalization effect is small and perturbative; (ii) nonrelativistic scaling region $\kappa_2 \ll k \ll \kappa_1$, the renormalization effect is large, while $c(\kappa) \gg v(\kappa)$ still holds; and (iii) relativistic scaling region $k \ll \kappa_2$, $c \cong v$ and the Lorentz invariance is recovered.

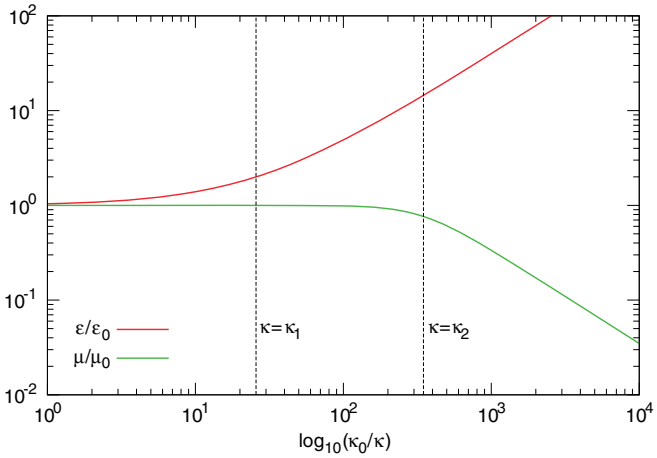

FIG. 3. (Color online) Analytic solutions to the RG equations for the permittivity ε and the permeability μ. The characteristic momentum scales are different for ε and μ.

D. Electromagnetic properties

Let us discuss the permittivity $\varepsilon(\kappa)$ and the permeability $\mu(\kappa) = 1 + 4\pi\chi$ (χ: magnetic susceptibility). The analytic solutions obtained from Eq. (11) and $\mu = 1/(\varepsilon c^2)$ are shown in Fig. 3. The momentum scale κ can be regarded as the temperature T by $T \cong v(\kappa)\kappa$. As noted above, the velocity $v(\kappa)$ is the function of the momentum scale, hence the energy dispersion $E(k) = v(k)k$ is a nonlinear function of k. From the definition of κ_1 and κ_2, $v(\kappa_1) \cong v_0$ and $v(\kappa_2) \cong c_\infty$, and the corresponding temperatures are estimated as $T_1 = T(\kappa_1) \cong v_0\kappa_1$ and $T_2 = T(\kappa_2) \cong c_\infty\kappa_2$. In Fig. 3, it can be seen that the permittivity $\varepsilon(\kappa)$ grows logarithmically below T_1 while the permeability $\mu(\kappa)$ decreases below T_2. The orbital magnetic susceptibility χ without the electron-electron interaction logarithmically diverges as a function of T, but in our analysis the logarithmic divergence is canceled due to the renormalization of v. These contrasting behaviors of ε and μ facilitate the identification of T_1 and T_2 experimentally. In the zero-temperature limit ε diverges while μ goes to zero (i.e., the perfect diamagnetism $\chi = -1/(4\pi)$ is accomplished).

E. Spectral function

For the physical interpretation of the electron Green's function, we should consider the self-energy in Coulomb gauge as discussed above. In Coulomb gauge,[15] the electron self-energy is

$$\Sigma(p) = -\frac{e^2/\varepsilon}{2\pi^2\epsilon}\frac{v^2}{c^3(c+v)^2}\gamma^0p_0 + \frac{e^2/\varepsilon}{6\pi^2\epsilon}\frac{1}{v(c+v)^2} \times\left[1+2\left(\frac{v}{c}\right)+\left(\frac{v}{c}\right)^2-\left(\frac{v}{c}\right)^3\right]v\vec{\gamma}\cdot\vec{p}. \tag{16}$$

In principle, ARPES can measure the energy dispersion $E(k) = v(\kappa = k)k$, which shows crossovers at κ_1 and κ_2. For the spectral function of electrons, the electron field renormalization is required, which is given by

$$\gamma_2(v,c,e^2/\varepsilon;\kappa) = \frac{1}{2}\kappa\frac{d\ln Z_{2t}}{d\kappa} = \frac{e^2/\varepsilon}{4\pi^2}\frac{v^2}{c^3(c+v)^2}. \tag{17}$$

From the Callan-Symanzik equation, the electron Green's function is modified by the momentum-scale-dependent functions $v(k)$, $\alpha(k)$, and $\gamma_2(k)$, then we obtain

$$G(\vec{k},\omega) = \frac{\mathcal{G}(\alpha(k))}{\omega^2 - v^2(k)\vec{k}^2} \exp\left[2\int_\Lambda^k d\ln\left(\frac{k'}{\Lambda}\right)\gamma_2(\alpha)\right], \quad (18)$$

where $k' = (\omega', v\vec{k}')$ is a four-momentum, Λ is the energy cutoff, and $\mathcal{G}$ is a function determined from a perturbative renormalization calculation.

In region (i), $\gamma_2 = 0$, so the Green's function is unchanged. In region (ii), κ dependence of γ_2 is rather complicated to calculate $G(\vec{k},\omega)$, so we only consider the relativistic scaling region (iii), where v approaches c and the original QED regime is applicable. When we put $c = v = c_\infty$, $\gamma_2(k)$ is expressed as

$$\gamma_2(k) = \frac{\alpha(k)}{16\pi^2} = \frac{\alpha_0}{16\pi^2}\frac{1}{1+\frac{\alpha_0}{6\pi^2}\ln\left(\frac{\Lambda}{k}\right)}, \quad (19)$$

and the perturbative correction for $\mathcal{G}$ is

$$\mathcal{G}(\alpha(k)) = 1 + \frac{\alpha(k)}{16\pi^2}\ln\left(\frac{e^\gamma}{4\pi}\right) + O(\alpha^2). \quad (20)$$

Then, the Green's function becomes

$$G(\vec{k},\omega) = \frac{\mathcal{G}(\alpha(k))}{\omega^2 - c_\infty^2\vec{k}^2}\frac{1}{\left[1+\frac{\alpha_0}{12\pi^2}\ln\left(\frac{\Lambda^2}{\omega^2 - c_\infty^2\vec{k}^2}\right)\right]^{3/4}}. \quad (21)$$

By substituting ω with $\omega + i0$, the imaginary part of the Green's function $-\mathrm{Im}G(\vec{k},\omega)$ gives the electron spectral function. The electron spectral function has finite value for $|\omega| < |\vec{k}|$, while $-\mathrm{Im}G(\vec{k},\omega) = 0$ outside that region. As depicted in Fig. 4, the perturbative correction for $\mathcal{G}$ gives very small contribution, so we put $\mathcal{G} = 1$ in the following analysis. When the bare coupling constant α_0^2 is small enough, the spectral function has the approximate form

$$-\mathrm{Im}G(\vec{k},\omega) \sim a\delta\left(\omega^2 - c_\infty^2\vec{k}^2\right) + \frac{\alpha_0}{32\pi c_\infty|\vec{k}|} \times\left(\frac{1}{c_\infty|\vec{k}| - \omega} + \frac{1}{c_\infty|\vec{k}| + \omega}\right), \quad (22)$$

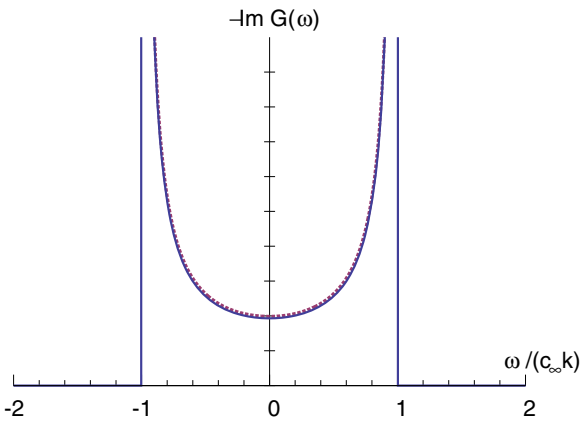

FIG. 4. (Color online) Frequency dependence of the density of states in region (iii) with $\alpha_0 = 1$. The vertical axis is in linear but arbitrary scale. The solid line denotes the result with the perturbative correction in $\mathcal{G}$, while the dashed line depicts the result for $\mathcal{G} = 1$.

where the residue a is a constant determined from the sum rule. The δ function peak with finite a means that the system remains a Fermi liquid in sharp contrast to the $(2+1)$D case,[10] while the continuum state for $|\omega| < c_\infty k$ comes from the interaction as shown in Fig. 4.

F. Energy gap

Up to now, we have focused on the critical point ($m = 0$), but the mass m is a relevant parameter. Experimentally, the bare mass m_0 can be controlled by the concentration x or by pressure P.[7,8] The RG equation for mass $m(\kappa)$ is

$$\kappa\frac{dm(\kappa)}{d\kappa} = -\frac{3\alpha(\kappa)}{8\pi^2}m. \quad (23)$$

Then, the mass at momentum scale p is

$$m(p) = m(\Lambda)\left[1+\frac{\alpha_0}{6\pi^2}\ln\left(\frac{\Lambda}{p}\right)\right]^{9/4}. \quad (24)$$

When we neglect the weak singularity with $\log\log m_0$, the solution to Eq. (24) is given by $m = m_0[1+\frac{\alpha_0}{6\pi^2}\ln(\frac{\Lambda}{m_0})]^{9/4}$, which describes the critical behavior of the gap as a function of $m_0 \propto (x - x_c)$ or $m_0 \propto (P - P_c)$ with x_c (P_c) being the critical concentration (pressure).

III. DISCUSSION AND SUMMARY

Now we discuss the relevance of the present results to the real systems. The velocity v_0 is estimated at $v_0 \cong 10^6$ m/s from the ARPES measurement of the energy dispersion,[7] hence $c_{\mathrm{vacuum}}/v_0 \cong 300$. As the dielectric constant, we take the typical value $\varepsilon_0 \cong 10^2$ for BiSb alloys.[16] Since $c_0 = c_{\mathrm{vacuum}}/\sqrt{\varepsilon_0}$, $c_0/v_0 \cong 30$, $(c_0/v_0)^{2/3} \cong 10$, and $\alpha_0 = (c_{\mathrm{vacuum}}/v_0) \times 1/137 \cong 3$ are obtained. These values give the estimates for $\kappa_1 \cong 10^{-8}\kappa_0$ and κ_2 being extremely small. Unfortunately, it would be difficult to observe the effect of electron-electron interaction and the scaling behavior at the experimentally accessible temperature in the materials at hand. However, there are many candidates for the correlated topological insulators recently proposed and partly synthesized.[17–28] The smaller value of v_0 rapidly (exponentially) increases κ_1, which gives the clue to look for the appropriate materials to study the scaling behavior of the quantum criticality.

In summary, we have studied the $(3+1)$D Dirac electrons coupled to electromagnetic field as the model for the quantum critical phenomenon of the transition between topological insulator and trivial insulator. The RG equations are derived and the two scaling regions are identified (i.e., the nonrelativistic and relativistic scaling regions). The Lorentz invariance is recovered in the latter case. The physical properties such as the the permittivity, the permeability, and the electron spectral function have been discussed based on the RG equations.

ACKNOWLEDGMENTS

The authors acknowledge the fruitful discussion with T. Hatsuda. This work is supported by a Grant-in-Aid for Scientific Research (Grant No. 24224009) from the Ministry of Education, Culture, Sports, Science and Technology of Japan, Strategic International Cooperative Program (Joint

Research Type) from Japan Science and Technology Agency, and Funding Program for World-Leading Innovative RD on Science and Technology (FIRST Program).

APPENDIX: PRECISION OF THE ANALYTIC SOLUTIONS

In the appendix, we consider the precision of the analytic solutions to the RG equations, especially the validity of the relation $c^2 v = \text{const}$. In this section, we define $x = 1 - v/c$, $y = c^2 v$. The RG equations for x, y and e^2/ε are

$$\kappa \frac{dx}{d\kappa} = \frac{e^2/\varepsilon}{12\pi^2} \frac{1}{y} f(x), \tag{A1}$$

$$\kappa \frac{dy}{d\kappa} = -\frac{e^2/\varepsilon}{6\pi^2} g(x), \tag{A2}$$

$$\kappa \frac{d(e^2/\varepsilon)}{d\kappa} = \frac{(e^2/\varepsilon)^2}{6\pi^2} \frac{1}{y}, \tag{A3}$$

where

$$f(x) = \frac{x(1-x)(24 - 34x + 12x^2 - x^3)}{(2-x)^2}, \tag{A4}$$

$$g(x) = \frac{x^2(1-x)^2}{(2-x)^2}. \tag{A5}$$

From Eqs. (A2), (A3), we obtain

$$\frac{e^2/\varepsilon}{y} \frac{dy}{d(e^2/\varepsilon)} = -g(x). \tag{A6}$$

We assume $v \leqslant c$, i.e. $0 \leqslant x \leqslant 1$, so that $0 \leqslant g(x) \leqslant 17 - 12\sqrt{2} \cong 0.03$. The RHS of Eq. (A6) is small, so the relative difference of y is

$$\frac{y(\kappa)}{y_0} \sim \left[\frac{(e^2/\varepsilon)(\kappa)}{e_0^2/\varepsilon_0} \right]^{-g(x)}. \tag{A7}$$

The maximum value $g(x) \cong 0.03$ is rarely observed. Thus, $y = c^2 v$ can be regarded as a constant to a large extent.

[1] For a description of quantum electrodynamics, see for example M. E. Peskin and D. V. Schroeder, *Introduction to Quantum Field Theory* (Westview, New York, 1995); P. Ramond, *Field Theory: A Modern Primer*, 2nd ed. (Addison-Wesley, New York, 1989).

[2] A. Damascelli, Z. Hussain, and Z.-X. Shen, Rev. Mod. Phys. **75**, 473 (2003).

[3] A. H. Castro Neto, F. Guinea, N. M. R. Peres, K. S. Novoselov, and A. K. Geim, Rev. Mod. Phys. **81**, 109 (2009).

[4] Y. Fuseya, M. Ogata, and H. Fukuyama, Phys. Rev. Lett. **102**, 066601 (2009), and references therein.

[5] M. Z. Hasan and C. L. Kane, Rev. Mod. Phys. **82**, 3045 (2010).

[6] X.-L. Qi and S.-C. Zhang, Rev. Mod. Phys. **83**, 1057 (2011).

[7] S.-Y. Xu, Y. Xia, L. A. Wray, S. Jia, F. Meier, J. H. Dil, J. Osterwalder, B. Slomski, A. Bansil, H. Lin, R. J. Cava, and M. Z. Hasan, Science **332**, 560 (2011).

[8] T. Sato, K. Segawa, K. Kosaka, S. Souma, K. Nakayama, K. Eto, T. Minami, Y. Ando, and T. Takahashi, Nature Phys. **7**, 840 (2011).

[9] V. N. Kotov, B. Uchoa, V. M. Pereira, F. Guinea, and A. H. Castro Neto, Rev. Mod. Phys. **84**, 1067 (2012).

[10] J. González, F. Guinea, and M. A. H. Vozmediano, Nucl. Phys. B **424**, 595 (1994).

[11] P. Goswami and S. Chakravarty, Phys. Rev. Lett. **107**, 196803 (2011).

[12] P. Hosur, S. A. Parameswaran, and A. Vishwanath, Phys. Rev. Lett. **108**, 046602 (2012).

[13] R. Shindou and S. Murakami, Phys. Rev. B **79**, 045321 (2009).

[14] We have dropped the θ term [i.e., $\theta \vec{E} \cdot \vec{B}$ ($\theta = \pm\pi$) in the action], which should be present in the topological insulator phase. This term, however, can be transformed into the surface term, and the sign of θ is determined by the time-reversal symmetry breaking on the surface. The topological magneto-electric effect is derived from this term, but this is beyond the scope of this present paper, where only the permittivity ε and the magnetic permeability μ are discussed.

[15] G. S. Adkins, Phys. Rev. D **27**, 1814 (1983).

[16] X.-L. Qi, R. Li, J. Zang, and S.-C. Zhang, Science **323**, 1184 (2009).

[17] A. Shitade, H. Katsura, J. Kuneš, X.-L. Qi, S.-C. Zhang, and N. Nagaosa, Phys. Rev. Lett. **102**, 256403 (2009).

[18] J. Chaloupka, G. Jackeli, and G. Khaliullin, Phys. Rev. Lett. **105**, 027204 (2010).

[19] H.-C. Jiang, Z.-C. Gu, X.-L. Qi, and S. Trebst, Phys. Rev. B **83**, 245104 (2011).

[20] J. Reuther, R. Thomale, and S. Trebst, Phys. Rev. B **84**, 100406 (2011).

[21] Y. Singh, S. Manni, J. Reuther, T. Berlijn, R. Thomale, W. Ku, S. Trebst, and P. Gegenwart, Phys. Rev. Lett. **108**, 127203 (2012).

[22] C. H. Kim, H. S. Kim, H. Jeong, H. Jin, and J. Yu, Phys. Rev. Lett. **108**, 106401 (2012).

[23] Y. Singh and P. Gegenwart, Phys. Rev. B **82**, 064412 (2010).

[24] X. Liu, T. Berlijn, W. G. Yin, W. Ku, A. Tsvelik, Y.-J. Kim, H. Gretarsson, Y. Singh, P. Gegenwart, and J. P. Hill, Phys. Rev. B **83**, 220403 (2011).

[25] S. K. Choi, R. Coldea, A. N. Kolmogorov, T. Lancaster, I. I. Mazin, S. J. Blundell, P. G. Radaelli, Y. Singh, P. Gegenwart, K. R. Choi, S.-W. Cheong, P. J. Baker, C. Stock, and J. Taylor, Phys. Rev. Lett. **108**, 127204 (2012).

[26] F. Ye, S. Chi, H. Cao, B. C. Chakoumakos, J. A. Fernandez-Baca, R. Custelcean, T. F. Qi, O. B. Korneta, and G. Cao, Phys. Rev. B **85**, 180403 (2012).

[27] D. Pesin and L. Balents, Nature Phys. **6**, 376 (2010); H.-M. Guo and M. Franz, Phys. Rev. Lett. **103**, 206805 (2009); B.-J. Yang and Y. B. Kim, Phys. Rev. B **82**, 085111 (2010); M. Kurita, Y. Yamaji, and M. Imada, J. Phys. Soc. Jpn. **80**, 044708 (2011); M. Kargarian, J. Wen, and G. A. Fiete, Phys. Rev. B **83**, 165112 (2011).

[28] D. Xiao, W. Zhu, Y. Ran, N. Nagaosa, and S. Okamoto, Nature Commun. **2**, 596 (2011).